JOURNAL OF APPLIED ELECTROCHEMISTRY 17 (1987) 1065–1074

Anodization of molybdenum. I. Galvanostatic anodization

A. G. GAD-ALLAH, H. A. ABD EL-RAHMAN

Department of Chemistry, Faculty of Science, Cairo University, Giza, Egypt

Received 3 November 1986; revised 12 February 1987

Molybdenum was anodized at different current densities (10^{-4}–10^{-2} A cm^{-2}) in various aqueous solutions. Potential–time curves obtained in strong acid solutions are similar to those usually reported for the valve metals, and the anodization kinetics were found to obey the familiar exponential law

$$i = A \exp BH$$

and also to obey the empirical relation,

$$(dE/dt)_i = a(i)^b$$

Using both polarization and capacitance measurements, it was found that the field strength, H, the electrolytic parameters A and B and the constants a and b are comparable with those previously reported for many valve metals. Except in strong acid solutions, E–time curves showed an induction period before oxide formation. The duration time of the induction period, t_i, was found to increase with decrease of solution acidity and current density and with increase of temperature. Although chloride ion may act as a depolarizer, t_i was found to decrease with increase of chloride ion concentration, probably by increasing the anodization field strength.

1. Introduction

Earlier work on the electrochemical behaviour of molybdenum showed that the metal is passivated by a thin oxide film of MoO_2 [1–4]. Using cyclic voltammetry Hull [5, 6] identified three films (MoO_2, MoO_3 and $Mo(OH)_3$) in KOH solutions and two films (MoO_2 and MoO_3) in H_2SO_4 solutions. The anodic dissolution of molybdenum in sulphates [7] and chloride solutions [8] was studied by Johnson *et al.* They suggested that the dissolution proceeds via further oxidation of MoO_2 to MoO_3. Our previous work on molybdenum [9, 10] showed that the metal is covered with a thin, insulating and capacitive film in practically all aqueous solutions. Wood and Pearson [11, 12] concluded that both molybdenum and vanadium cannot normally be anodized. However, Keil and Ludwig [13] found that vanadium can be anodized in concentrated acetic acid saturated with sodium borate. The few experiments due to Ikonopisov [14] are, perhaps, the only successful anodization experiments to produce insulating anodic films on molybdenum to appreciable voltages ($\simeq 300$ V). Ikonopisov concluded that the kinetics of anodization were appreciably different from those usually observed. Recently, we succeeded in producing true insulating anodic films on molybdenum by anodization in strong acid solutions [15]. As will be seen in this paper the anodization kinetics in strong acid solutions are similar to those of valve metals. In Part II [16] the electrical breakdown and post-breakdown anodization experiments will be discussed.

2. Experimental details

A molybdenum disc electrode of apparent surface area ~ 0.125 cm^2 was cut from spec. pure molybdenum rod (Johnson–Matthey, London). The electrode preparation, electrolytic cell, electric circuit and details of the experimental procedure have been described previously [9, 17].

0021–891X/87 $03.00 + .12

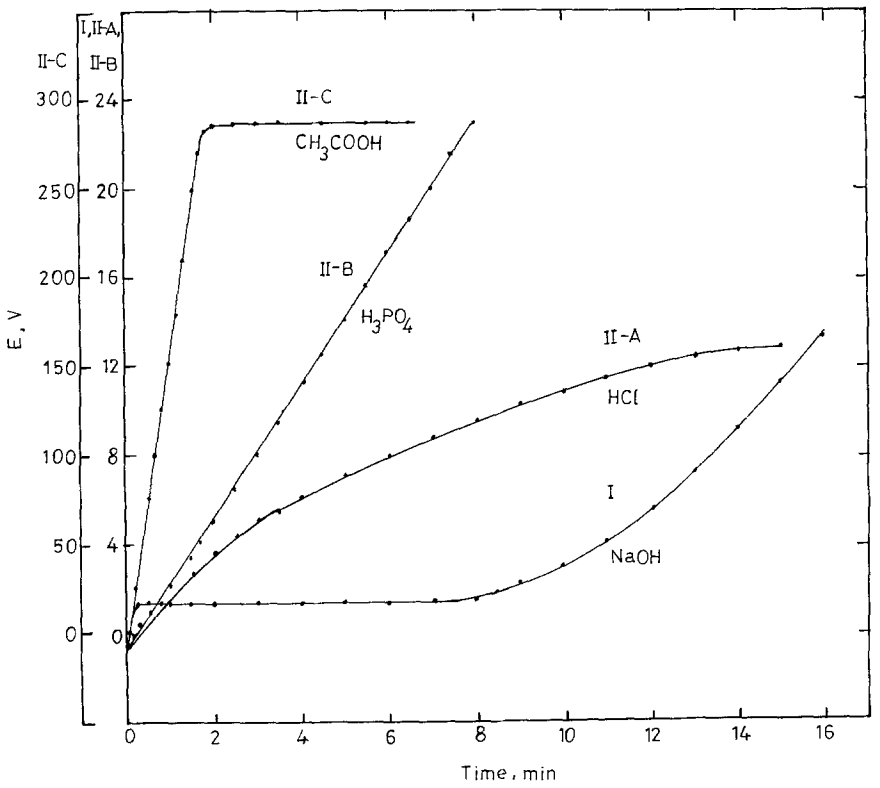

Fig. 1. Potential–time curves for molybdenum in molar solutions of NaOH, HCl, H_3PO_4 and acetic acid at current densities of 1.6, 0.2, 0.2 and 8.0 mA cm^{-2}, respectively.

All solutions were prepared from AnalaR grade chemicals and triply distilled water. The experiments were carried out in an air thermostat of temperature 30 ± 0.2° C. The capacitance of the electrode was measured at 1 kHz and the electrode potential was measured against a saturated calomel electrode (SCE). The buffer solutions prepared were from the modified universal buffer mixture (Briton and Robinson) and checked using a pH meter.

3. Results and discussion

3.1. *General anodization behaviour*

Molybdenum was anodized at constant current density in the range of 10^{-4} to 10^{-2} A cm^{-2} in various aqueous solutions. The general anodization behaviour is illustrated in Fig. 1. Curve I represents the general behaviour in weak acid, neutral and alkaline solutions. Curve II-A represents the behaviour in hydrohalic acids, whereas curve II-B represents that in other strong acid solutions, e.g. H_3PO_4, H_2SO_4, HNO_3. . . etc. Curve II-C represents the behaviour at high current density in any electrolyte. The distinct difference between curves I and II is the presence of a potential arrest in curve I. Such arrest was previously reported for Mo [14], W [18], Bi [19], Sb [20, 21], V [22] and Al [23] and referred to as the 'induction period'. The anodization of molybdenum was found to yield coloured films characteristic of the formation voltage reached during the anodization as in the case of valve metals.

It is assumed that the following processes occur during the anodization of molybdenum: (i) metal dissolution; (ii) oxide formation; and (iii) oxygen and/or halogen evolution. In acetic acid solutions of pH 5 the oxide formation efficiency was estimated to be 72%, assuming that metal dissolution and oxide formation are the only anodic processes [24]. However, under anodization at high current density, as in our case, oxygen evolution can be seen by the naked eye. During the linear increase of potential with

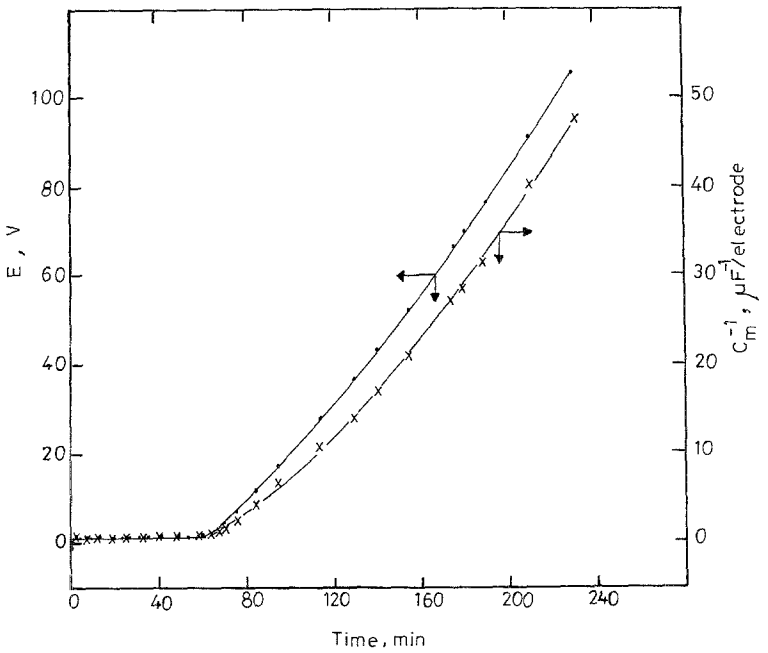

Fig. 2. Variation of potential, E, and reciprocal capacitance, C_m^{-1}, of molybdenum electrode with time of anodization at a current density of 0.8 mA cm^{-2} in 0.2 M NaOH solution.

time (curves II-A, II-B and II-C), the oxide formation predominates over the other anodic processes and is assumed to proceed with about 100% efficiency. Then, oxygen evolution and the other anodic processes are involved. During the induction period (curve I) oxygen evolution and the other anodic processes are predominant and oxide formation is negligible. The electrode capacitance, C_m, was measured during the anodization and it was found that: (i) C_m is constant during the induction period; (ii) C_m^{-1} increases linearly with formation voltage increase (see Figs 2, 3).

3.2. *Nature of the induction period*

As can be seen from Figs 4 and 5 the duration of the induction period, t_i, was found to

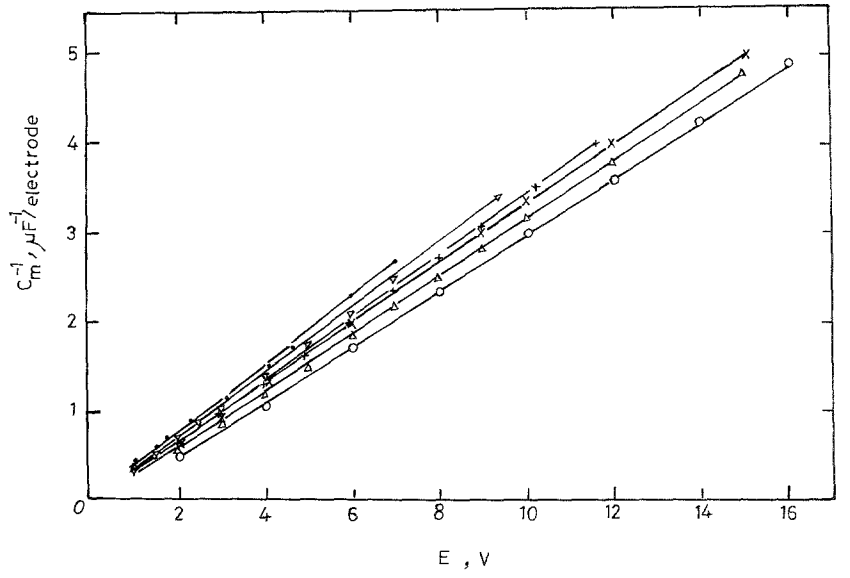

Fig. 3. Reciprocal capacitance–potential relations for molybdenum in 1.0 M HCl solution at the following anodizing current densities (μA cm^{-2}) of: ●, 26; ▽, 120; +, 200; ×, 600; △, 1200; ○, 2000.

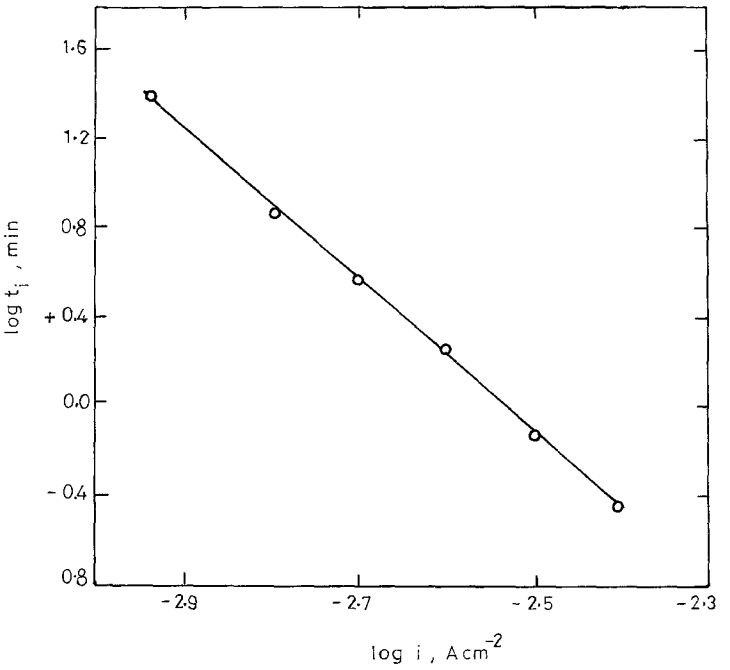

Fig. 4. Variation of logarithm of induction time t_i, with logarithm of current density of anodization of molybdenum in 1.0 M NaOH solution.

decrease with increase of current density and with decrease of temperature in agreement with the behaviour previously reported for many valve metals [14, 18–23]. To clarify the effect of the anodizing electrolyte on t_i the effect of both pH and chloride ion concentration was studied. As can be seen in Fig. 6, the decrease of pH reduces t_1. Fig. 7 also shows that the increase of chloride ion concentration decreases t_i. The latter finding was not expected due to the known aggressive action of chloride ion and due to the ability of chloride ion to act as a depolarizer [25]. Both reasons were expected to delay the oxide formation, i.e. t_1 increases. However, the known aggressive action of the chloride ion on many metals can be excluded in the case of molybdenum since molybdenum oxide films are insoluble in chloride solutions [1]. All the previous explanations of the induction period were based on the assumption of the existence of a critical value of the anodizing current density [18, 19] below which the induction period appears. In their model on bismuth, Ikonopisov and Nikolov [19] explain the dependence of t_i on current density, temperature and oxalic acid concentration by assuming the precipitation of crystals of a slightly soluble bismuth compound which isolate a part of the electrode surface. When the current density on the uncovered surface reaches the critical value an anodic film begins to grow on it. According to that model the increase of current density increases the rate of surface coverage and hence the critical current density is reached faster, i.e. a t_i decrease occurs. The increase of temperature increases the solubility of the precipitated film and hence t_i increases. The increase of acidity causes faster dissolution of the precipitated film, i.e. t_i increases.

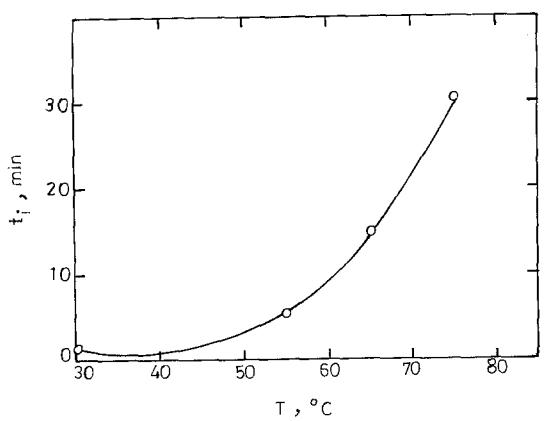

Fig. 5. Variation of induction time, t_i, with temperature of anodization of molybdenum in 0.2 M NaOH solution.

Although the previous model can be applied for many cases, it is not applicable in the case of molybdenum because it can not explain the

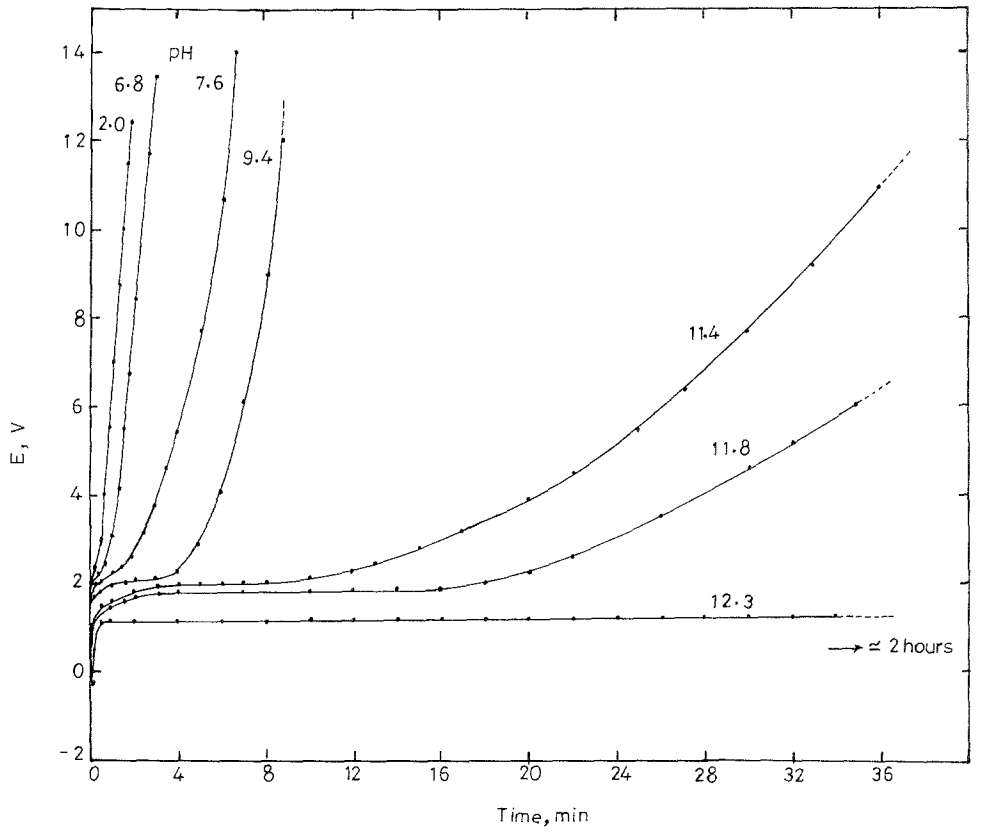

Fig. 6. Potential–time curves for molybdenum at a current density of 0.8 mA cm^{-2} in buffer solutions of pH: 2, 6.8, 7.6, 9.4, 11.4, 11.8 and 12.3.

increase of t_i with pH increase. The induction period for molybdenum can be explained as follows. At the beginning of the anodization the metal is covered either with an oxide film via the dissolution process [6],

$$Mo + H_2O = MoO^+ + 2H^+ + 3e$$

$$MoO^+ + H_2O = MoO_2(s) + 2H^+ + e$$

or more probably via water oxidation,

$$2H_2O = O_2 + 2H^+ + 4e$$

$$Mo + O_2 = MoO_2(s)$$

Then oxide formation and/or other anodic processes (oxygen evolution and metal dissolution) occur. As the solution pH increases the probability of oxygen evolution increases and oxide formation is retarded. Since oxygen evolution is accompanied by a decrease of the solution pH in the vicinity of the metal surface, it may be expected that after a certain time, t_i, a critical pH is reached after which oxide formation occurs and, hence, t_i is expected to decrease with pH decrease. Also, the increase of current density accelerates hydrogen ion production and, hence, reduces t_i. The effect of current density, tem-

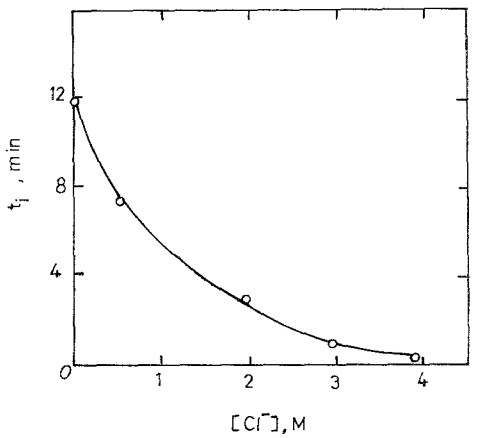

Fig. 7. Variation of induction time, t_i, with chloride ion concentration for anodization of molybdenum at a current density of 0.8 mA cm^{-2} in chloride-containing solutions at pH 12.

perature and chloride ion concentration on t_i may be explained on the basis that these factors affect the anodization field strength as will be discussed later.

3.3. *Anodization kinetics*

In galvanostatic anodization, the total anodic current density, i_a, is the sum of the ionic current density, i, the electronic current density, i_e, and the current density of dissolution of the oxide in the steady state, i_s [26], thus

$$i_a = i + i_e + i_s \quad (1)$$

Generally, one may write

$$i = Bi_a \quad (2)$$

where $B \leqslant 1$. The anodization process proceeds via the moving of ions in the direction of the associated electric field. The simplest relation between the electric field strength, H, and the ionic current density is the familiar Günther-schulze and Betz relationship [27, 28],

$$i = A \exp BH \quad (3)$$

where A and B are constants usually called electrolytic parameters, and

$$H = (dE/dx)_i \quad (4)$$

where E is the electrode potential and x is the film thickness. Values of H can be estimated from potential–thickness relations by using coulometry, ellipsometry or capacitance measurements for thickness determination [29].

The coulometric determination of the film thickness increase, dx, is applied only when the oxide formation proceeds with a known efficiency. Assuming 100% efficiency [26],

$$dx = (M/a\sigma snF)It = rIt/a\sigma \quad (5)$$

where M is the molecular weight of the oxide, s its density, n the number of Faradays (F) required for the formation of one mole of oxide, σ is a roughness factor, r is the volume of oxide in cm^3 formed per coulomb, I is the current intensity (A), and t is the time of polarization from the beginning. Taking M of MoO_2 equal to 127.94, $s = 6.4\,g\,cm^{-3}$ [30], $n = 4$ and $a = 0.125\,cm^2$, the field determined by this method, H_1, is given by

$$H_1/\sigma = 1/ri(dE/dt)_i \quad (6)$$

where the field is expressed as H_1/σ to eliminate the uncertainty in σ.

The film thickness can be estimated from capacitance measurements by applying the relationship for a parallel plate condenser, $C_m = \varepsilon a/4\pi \times 9 \times 10^5 x$, thus:

$$dx = (\varepsilon\sigma a/4\pi \times 9 \times 10^5)dC_m^{-1} \quad (7)$$

where C_m is the measured capacitance in μF and ε is the dielectric constant. Assuming that $\varepsilon = 29.4$ [31], the field was denoted H_2, and estimated thus:

$$\sigma H_2 = \frac{4\pi \times 9 \times 10^5}{\varepsilon\sigma a}(dE/dC_m^{-1})_i \quad (8)$$

Due to the uncertainty in the surface area, it is preferred to determine the thickness by a method independent of the surface area. Combining Equations 5 and 7 and taking the square root of both sides yields

$$dx = (\varepsilon r/4\pi \times 9 \times 10^5)^{-1/2}(QdC_m^{-1})^{1/2} \quad (9)$$

where $Q = It$ in coulombs. The field determined by this method is denoted H_3, and estimated thus:

$$H_3 = (\varepsilon r/4\pi \times 9 \times 10^5)^{-1/2}(dE/(QdC_m^{-1})^{1/2})_i \quad (10)$$

Actually, H_3 is the geometric mean of both H_1 and H_2 and, hence, the roughness factor, σ, can be estimated either by dividing H_3 by the field obtained from coulometry or by dividing the field obtained from capacitance by H_3.

Yahalom and Hoar [32] derive Equation 3 on the basis of the theory of rate processes as:

$$i = zF(kT/h)(n/N)\exp(-\Delta G_0^*/RT) \times \exp(zFa^*H/RT) \quad (11)$$

where z is the valency of the mobile ion, n is the number of charge carriers per cm^2, ΔG_0^* is the standard free energy of activation for the ionic jump in the absence of field, a^* is the effective activation distance and N, h, k, T and R have their usual meanings. A comparison of Equations 3 and 11 shows that

$$A = zF(kT/h)(n/N)\exp - \Delta G_0^* \quad (12)$$

and

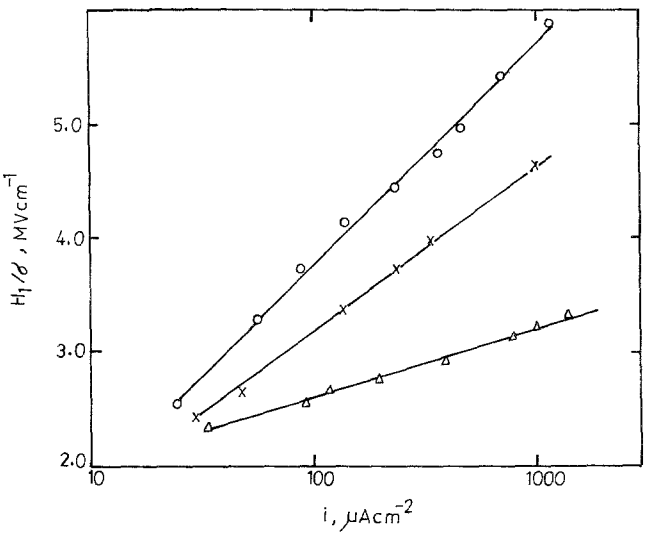

Fig. 8. H_1/σ versus log i relations for molybdenum in molar solutions of: ○, H_3PO_4; ×, H_2SO_4; △, HCl.

$$B = zFa^*/RT \quad (13)$$

Taking the logarithm of both sides of Equation 3 and rearranging yields:

$$H = 2.303/B \log i - 2.303/B \log A \quad (14)$$

The validity of Equation 14 for molybdenum was tested in molar solutions of H_3PO_4, H_2SO_4 and HCl by applying the previous three methods, and is shown in Figs 8–10. The parameters A and B and the effective activation distance, a^*, were calculated and are given with those of some valve metals in Table 1. Also, the electric field

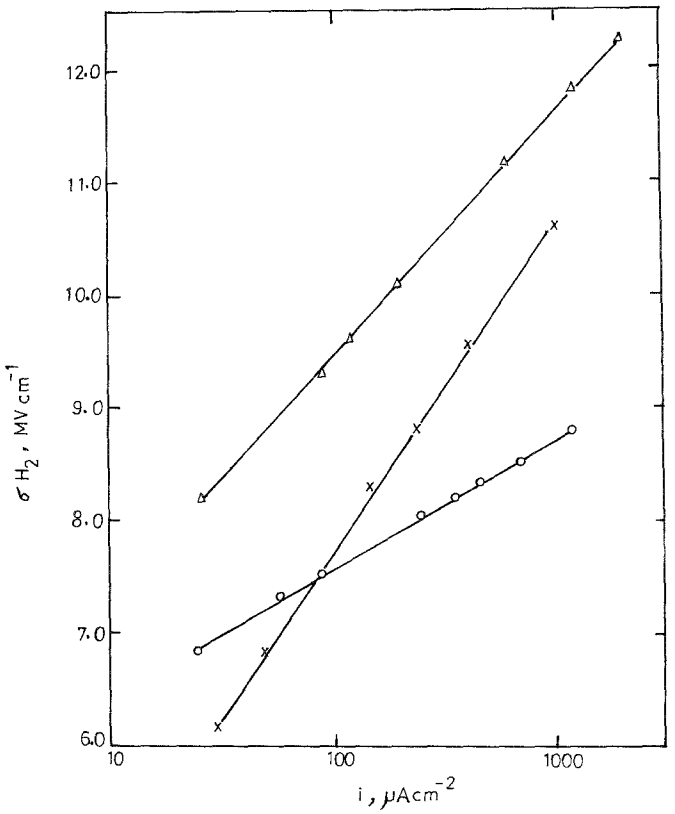

Fig. 9. σH_2 versus log i relations for molybdenum in molar solutions of: ○, H_3PO_4, ×, H_2SO_4; △, HCl.

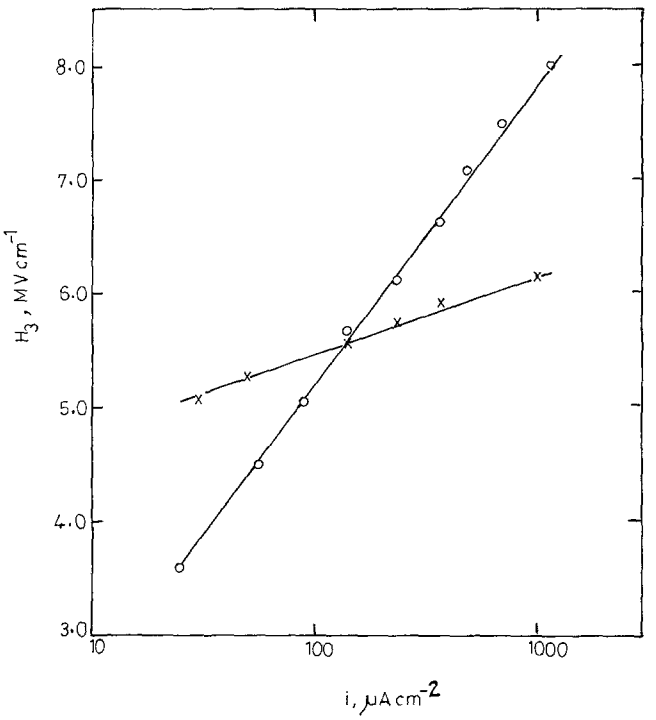

Fig. 10. H_3 versus log i relations for molybdenum in molar solutions of: ○, H_3PO_4; ×, H_2SO_4.

strengths are given in Table 2. The data given in Tables 1 and 2 show that the kinetic parameters of anodization of molybdenum are comparable with those of valve metals.

For most valve metals the formation rate, dE/dt, is related to the anodizing current density, i, by the empirical relation [26]:

$$(dE/dt)_i = a(i)^b \quad (15)$$

or

$$\log (dE/dt)_i = \log a + b \log i \quad (16)$$

where a and b are constants. The validity of Equation 16 in molar solutions of H_3PO_4, H_2SO_4 and HCl is shown in Fig. 11. The constants a and b are given with those of some valve metals in Table 3. As can be seen, both constants in the case of molybdenum are comparable with those of the rest of the metals.

The roughness factor, σ, was estimated in the solutions tested and the average value was found to be 1.5.

Table 1. Electrolytic parameters and effective activation distance

Metal	*Solution*	A ($A\,cm^{-2}$)	σB ($cm\,V^{-1}$)	σa^* (Å)
Mo	1.0 M H_2SO_4	73.6×10^{-6}	1.58×10^{-6}	1.03
	1.0 M H_3PO_4	1.0	1.19	0.78
	1.0 M HCl	0.0004	4.41	2.80
Nb	0.1 M H_2SO_4	2.3	1.70	0.85
	0.1 M H_3PO_4	13.4	1.00	0.50
Ta	0.1 M H_3PO_4	0.014	1.80	0.90
Al	0.1 M H_2SO_4	7.4	7.90	6.60
Sb	0.05 M H_2SO_4	17.0	2.10	1.70
	0.03 M H_3PO_4	0.41	3.50	2.90
Bi	0.05 M borate	4.1	3.90	3.20

All data are obtained, except for Mo, from [23]. Data for molybdenum are calculated by the first method (coulometry).

Table 2. Effective field strength at 30° C

Metal	*Solution*	*Current density* ($\mu A\,cm^{-2}$)	H ($V\,cm^{-1}$)
Mo	1.0 M H_2SO_4	30	2.42×10^6
	1.0 M H_3PO_4	25	3.27
	1.0 M HCl	35	2.36
W	0.5 M H_2SO_4	100	9.00
Ta	0.1 M H_3PO_4	5	6.60
Al	0.1 M borate	10	3.60
Bi	0.05 M H_2SO_4	1000	2.00
Sb	0.05 M H_2SO_4	60	0.60
Ti	1.0 M H_3PO_4	10	7.40
Zr	0.1 M H_3PO_4	10	3.80

All data, except for molybdenum, are extracted from [23]. Field strengths for molybdenum are calculated by the coulometric method.

Table 3. Constants of the empirical relation

Metal	*Solution*	a	b	Ref.
Mo	1.0 M H_2SO_4	1.0×10^3	1.20	
	1.0 M H_3PO_4	1.1×10^3	1.20	
	1.0 M HCl	2.1×10^2	1.04	
W	0.5 M H_2SO_4	1.2×10^4	1.42	[23]
	1.0 M $HClO_4$	2.0×10^3	1.27	[23]
Ta	0.1 M H_3PO_4	2.2×10^3	1.20	[23]
Nb	0.1 M $NH_4H_2PO_4$	4.1×10^2	1.10	[23]
Sb	0.1 M H_3PO_4	2.0×10^3	1.43	[23]
Bi	0.05 M Na_2SO_4	2.4×10^2	1.17	[23]
Zr	0.1 M H_3PO_4	2.2×10^2	1.06	[23]
Hf	0.5 M H_2SO_4	3.2×10^2	1.03	[29]

3.4. *Field strength effect on* t_i

The previous idea [19] of the existence of a critical current density for oxide formation may be better understood by taking into consideration the fact that oxide formation is controlled by the strength of the anodization field. As can be seen from Equation 11, the field strength increases with current density increase and with temperature decrease, which is the same behaviour of t_i with current density and temperature, i.e. the increase of anodization field reduces the time of the induction period. The dependency of t_i on H may be supported by the results in chloride solutions, where the increase of chloride ions was found to reduce t_i and to increase H (cf. Figs 7, 12).

Fig. 12 illustrates the variation of field strength, estimated from coulometry and capacitance measurements, versus chloride ion concentration. As can be seen, the field strength

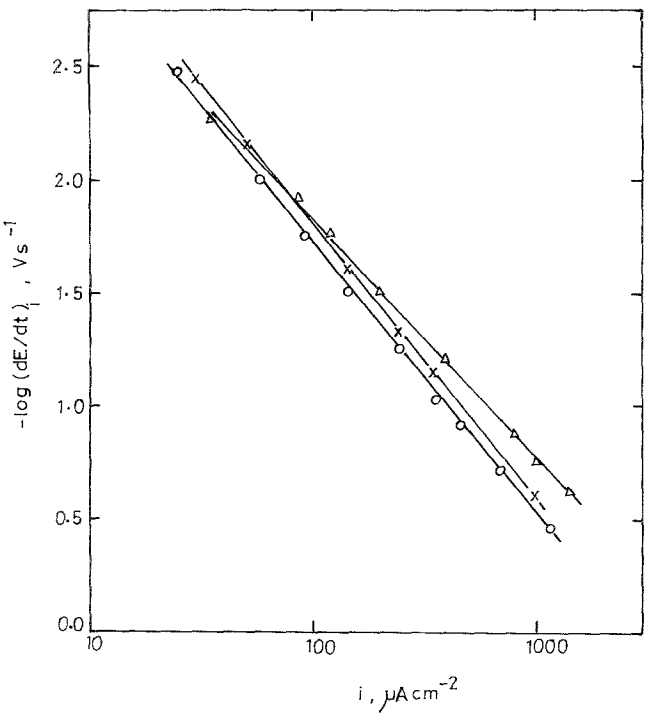

Fig. 11. Relation between the logarithm of formation rate and log i for molybdenum in molar solutions of: ○, H_3PO_4; ×, H_2SO_4; △, HCl.

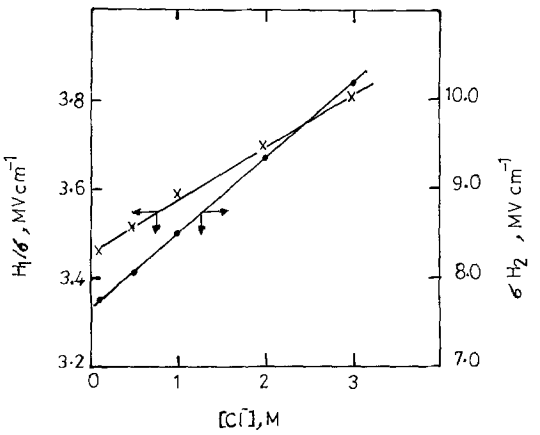

Fig. 12. Variation of both H_1/σ and σH_2 with chloride ion concentration for anodization of molybdenum at a current density of 114 μA cm^{-2} in solutions of 1 M H_2SO_4 + x M NaCl (●) Hi/σ; (×) σ H_2.

increases linearly with increase of chloride ion concentration probably due to incorporation of chloride ions during the oxide film formation. The incorporation of anions during the anodization of valve metals is well known [34–36] and the extent of incorporation is a function of concentration [36].

Acknowledgement

The authors would like to thank Professor Dr M. M. Abou-Romia for continuous support and valuable advice.

References

[1] T. Heumann and G. Hauck, *Z. Metallk.* **56** (1965) 75.
[2] L. L. Wikstrom and Ken Nobe, *J. Electrochem. Soc.* **116** (1969) 525.
[3] H. Nobuyoshi and S. Katsushisa, *Nippon Kinzoku* **44** (1980) 1312.
[4] J. N. Wanklyn, *Corr. Sci.* **21** (1981) 211.
[5] M. N. Hull, *J. Electroanal. Chem.* **30** (1971) App. 1.
[6] *Idem, ibid.* **38** (1972) 143.
[7] J. W. Johnson, C. H. Chi, C. K. Chen and W. J. James, *Corrosion* **26** (1970) 238.
[8] J. W. Johnson, M. S. Lee and W. J. James, *ibid.* **26** (1970) 507.
[9] W. A. Badawy, A. G. Gad-Allah, H. A. Abd El-Rahman and M. M. Abou-Romia, *Surface Technol.* **27** (1986) 187.
[10] A. G. Gad-Allah, W. A. Badawy, H. A. Abd El-Rahman and M. M. Abou-Romia, *ibid.*, in press.
[11] G. C. Wood and C. Pearson. *Corr. Sci.* **7** (1967) 119.
[12] *Idem, ibid.* **9** (1969) 367.
[13] R. G. Keil and K. Ludwig, *J. Electrochem. Soc.* **118** (1971) 864.
[14] S. Ikonopisov, *J. Electroanal. Chem.* **35** (1972) App. 1.
[15] H. A. Abd El-Rahman, MSc Thesis, Cairo University (1986).
[16] H. A. Abd El-Rahman, A. G. Gad-Allah and M. M. Abou-Romia, *J. Appl. Electrochem.* **17** (1987) 899.
[17] M. S. El-Basiouny, M. M. El-Kot and M. M. Hefny, *Br. Corros. J.* **14** (1979) 51.
[18] I. A. Ammar and R. Salim, *Corr. Sci.* **11** (1971) 591.
[19] S. Ikonopisov and Ts. Nikolov, *J. Electrochem. Soc.* **119** (1972) 1544.
[20] S. Ikonopisov, A. Girginov and V. Tsochev, *Compt. Rend. Acad. Bulg. Sci.* **25** (1972) 653.
[21] I. A. Ammar and A. Saad, *J. Electroanal. Chem.* **34** (1972) 159.
[22] R. G. Keil and R. E. Salomon, *J. Electrochem. Soc.* **115**, (1968) 628.
[23] S. Ikonopisov and L. Andreeva, *ibid.* **120** (1973) 1361.
[24] T. Nakamura and S. Haruyama, *Denki Kagaku* **48** (1980) 406.
[25] M. S. El-Basiouny, A. M. Bekheet and A. G. Gad-Allah, *Corrosion* **40** (1984) 116.
[26] I. A. Ammar, S. Darwish and M. W. Khalil, *Z. Werkstofftech.* **12** (1980) 421.
[27] A. Güntherschulze and H. Betz, *Z. Phys.* **92** (1934) 367.
[28] *Idem*, 'Elektrolyt-Kondensatoren', Kraya, Berlin (1937).
[29] L. Young, 'Anodic Oxide Films', Academic Press, London (1961).
[30] J. W. Meller, 'A Comprehensive Treatise on Inorganic and Theoritical Chem', Longmans, Vol. XI, (1948) p. 527.
[31] D. J. Desmet and J. L. Ord, *J. Electrochem. Soc.* **130** (1983) 280.
[32] J. Yahalom and T. P. Hoar, *Electrochim. Acta* **15** (1970) 877.
[33] M. S. El-Basiouny, A. M. El-Kot and M. M. Hefny, *Corrosion* **36** (1980) 284.
[34] J. J. Randall, W. J. Bernard and R. R. Wilkinson, *Electrochim. Acta* **10** (1965) 183.
[35] G. T. Roger, P. H. G. Draper and S. S. Wood, *ibid.* **13** (1968) 251.
[36] I. Montero, J. M. Albella and J. M. Martinez-Duart, *Electrochem. Soc.* **132** (1985) 814.